Translating Grid Code Requirements Into Control Design For Grid-Forming MMCs Under AC Faults

*†Xiaoxiao Liu, †Paul Judge, *Geraint Chaffey, *Dirk Van Hertem
*Dept. of Electrical Engineering, KU Leuven/Etch-EnergyVille, Leuven/Genk, Belgium
†School of Engineering, University of Edinburgh, Edinburgh, United Kingdom
xiaoxiao.liu@kuleuven.be, paul.judge@ed.ac.uk, geraint.chaffey@kuleuven.be, dirk.vanhertem@kuleuven.be

***Abstract*—Grid-following (GFL) converters are facing increasing challenges in weak and renewable-rich grids. As a result, grid-forming (GFM) converters are becoming a promising solution for future converter-dominated systems due to their ability to form grid voltage and frequency. Existing grid codes are largely made to standardise the behaviour of GFL converters, while it is unclear whether they can be applied to GFM. In recent years, system operators have begun introducing GFM-specific grid code that requires fast fault current injection, voltage support, and robust phase tolerance. However, it remains unclear how such requirements should be translated into practical GFM control design. This paper addresses this gap by analysing different current limiter methods, including reactive, active, and voltage-based priorities, and the influence of virtual impedance and voltage loop bandwidth on meeting grid code performance. Case studies show that prioritising positive and negative sequence currents improves voltage magnitude and symmetry. The results provide design guidelines linking grid code objectives to the control design of GFM MMCs.**

***Index Terms*—grid forming, MMC, grid code, AC faults**

I. Introduction

The rapid transition towards renewable-dominated energy introduces top-down changes to the power system. In large-scale applications, where bulk power must be transmitted over long distances, power electronics converters, particularly Modular Multilevel Converters (MMCs), have become standardized due to their high efficiency, scalability, and modularity [1]. Traditionally, grid-following (GFL) converters have been the mainstay in power systems featuring synchronous machine dominance. In GFL operation, the converter synchronizes to the existing grid voltage and frequency via a phase-locked loop (PLL). The PLL continuously measures the grid voltage phase angle and frequency, enabling the converter to work in a current source mode. While this control approach works well when there is a strong grid to "follow," it increasingly faces limitations in the low-inertia or weak-grid scenarios prevalent in renewable-rich networks [2].

Grid-forming (GFM) converters offer an alternative approach by acting more like a voltage source behind an impedance. Rather than relying on grid conditions to synchronise, GFM converters can establish voltage and frequency references independently, effectively "forming" the grid. This functionality emulates the behaviour of traditional synchronous machines, allowing the GFM converter to support grid stability more robustly during network disturbances [3].

The fault response in a synchronous generator-based power system is decided by the physical characteristics of the generator, while it is dominated by the converter control methods in a converter-dominated system. Grid codes are developed to standardise the response of control to ensure stable operation under various system conditions. All grid codes require that converters remain connected to the grid under voltage dips and inject reactive current to support the grid voltage [4]. Most of the national grid codes require the converter to inject negative-sequence reactive current under unbalanced grid conditions [5]. However, the existing grid codes have only been made and tested with GFL converters; whether they can be applied to GFM converters is unclear. Considering the natural difference between GFL and GFM, grid codes on GFM converters are required and assessed, specifically towards the voltage support and current injection ability.

In recent years, system operators and standards bodies worldwide have begun introducing GFM-specific grid code provisions that go beyond traditional GFL requirements [6]. Unlike GFL units that follow grid voltage and contribute limited fault current, GFM converters are required to actively regulate voltage and support the grid during transients. For instance, Great Britain's GC0137 mandates fast fault current injection (¡5 ms), phase-jump tolerance (up to 60°), and reactive prioritisation under voltage dips [7]. Australia's AEMO defines core functional tests for GFMs [8], while ENTSO-E and ACER work toward harmonised European specifications [9], [10]. Similarly, VDE FNN in Germany advances rules on instantaneous reserve and voltage support [11], and NERC and DOE in North America specify fast fault response, damping, and negative-sequence support [12], [13].

Nevertheless, these updated specifications remain at a relatively high level, and their practical impact depends on how converter controls are actually designed and tuned. To ensure compliance, it is necessary to interpret the code requirements in terms of control objectives, identify the relevant parameters that govern fault response, such as current limiting strategies, voltage control, and virtual impedance settings. Only by linking grid-code provisions to concrete control design choices can we determine feasible parameter ranges and guarantee that grid-forming converters consistently deliver the mandated support under AC faults.

This work is funded by the Global Ph.D. Partnership between KU Leuven and the University of Edinburgh, and "Innovative solutions for underground high-voltage lines and networks" funded by the Flemish Government.

979-8-3315-8138-1

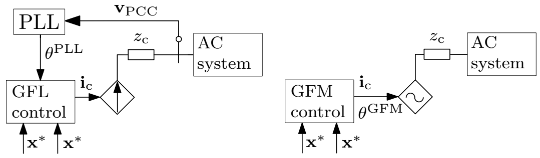

(a) GFL control (b) GFM control

Fig. 1. Fundamental difference between converters in GFL and GFM mode.

Building on this context, this paper compares different current limitation approaches and evaluates their ability to comply with recent grid-forming grid code requirements. Furthermore, the analysis extends to the parameterisation of the voltage controller and the virtual impedance, highlighting how their tuning influences fault current injection and providing suggestions on the grid code specifications. By systematically relating limiter behaviour and parameter design to grid-code provisions, the paper provides practical insights into selecting appropriate strategies and grid codes.

The remainder of this paper is organized as follows. Section II reviews the fundamental principles of GFM MMC operation, including synchronization, voltage control and current limitation. Section III examines existing grid codes, identifying potential gaps and how they might be addressed for GFM converters. The case study is provided in Section IV to discuss the effects of voltage support under different current limiters and the parameter study of fault current injection performance.

II. Fundamentals of GFM Converters

Under normal operating conditions, GFM regulates the terminal voltage and frequency to establish a stable grid reference. The fundamental difference between GFL and GFM converters is illustrated in Fig. 1, where GFL operates as a controlled current source and relies on an external grid to build the voltage, while GFM can be considered as a controlled voltage source behind an impedance [2].

Virtual synchronous machine (VSM) control is commonly used for synchronisation of GFM converters, which emulates the swing equation of synchronous machines (SMs) [14]. Voltage control is used to control the terminal voltage, and steady-state virtual impedance is used for shaping the equivalent impedance of the converter and limiting fault current. However, using virtual impedance alone cannot limit the transient fault current due to the low bandwidth of voltage control; direct current limitation is needed to improve current limitation performance [15]. VSM synchronisation, voltage control, virtual impedance, and direct current limitation used in this paper are introduced in this section.

A. VSM Synchronization

The virtual synchronous machine control emulates the electromechanical dynamics of a synchronous generator to provide a stable voltage and frequency reference in converter-dominated systems. The control structure is shown in Fig. 2. The controller emulates the swing equation as described in:

$$2H_{\mathrm{VSM}}\frac{d\omega_{\mathrm{VSM}}}{dt} = \begin{aligned} &p^*_{\mathrm{AC}} - K_\omega(\omega^*_{\mathrm{VSM}} - \omega_{\mathrm{VSM}}) \\ &- p_{\mathrm{AC}} - K_d(\omega_{\mathrm{VSM}} - \omega_{\mathrm{PLL}}) \end{aligned}, \tag{1}$$

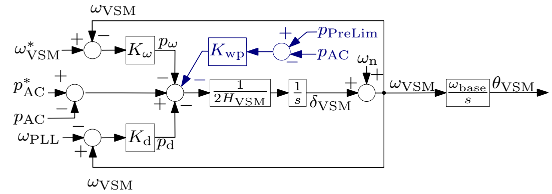

Fig. 2. Virtual synchronous machine control structure [14] [17].

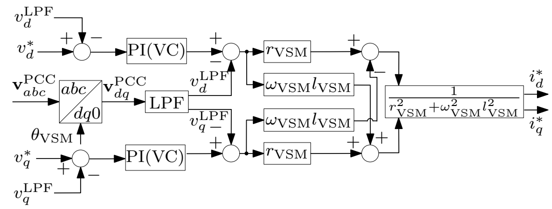

Fig. 3. Voltage control and virtual impedance to generate current reference.

where p^*_{AC} is the a power reference and p_{AC} is the measured active power from the converter to the grid. $K_d(\omega_{\mathrm{VSM}}-\omega_{\mathrm{PLL}})$ is the damping power. The mechanical time constant in the synchronous generator corresponds to $2H_{\mathrm{VSM}}$. A frequency controller is included and characterized by $K_\omega(\omega^*_{\mathrm{VSM}} - \omega_{\mathrm{VSM}})$. As a consequence, the virtual input power to the VSM swing equation is given by the sum of the external power reference and the frequency droop effect.

Under AC faults, the actual active power cannot reach the power reference due to current limitation. This difference between the power reference and the measured power will cause a frequency increase and an angle shift. Typical ways to solve this problem are to freeze the angle when the current is limited [16]; however, this might cause instability during fault recovery due to the long-period accumulation of power mismatch. Therefore, an anti-windup loop is added in the VSM control highlighted in blue in Fig. 2, which has been validated in [17]. The antiwindup feedback subtracts the difference between the saturated power p_{AC} and the unconstrained control action described by p_{PreLim}.

B. Voltage Control and Virtual Impedance

The internal voltage reference is provided by using voltage control and can be calculated by:

$$e^{dq}(s) = G_{\mathrm{v}}(s)(\begin{bmatrix} v_d^* \\ v_q^* \end{bmatrix} - H_{\mathrm{LPF}}(s)\begin{bmatrix} v_d^{\mathrm{PCC}} \\ v_q^{\mathrm{PCC}} \end{bmatrix}), \tag{2}$$

where $G_{\mathrm{v}}(s)$ is the PI controller of voltage control and H_{LPF} is a second-order long-pass filter, which are described by:

$$G_{\mathrm{v}}(s) = K_p^{\mathrm{v}} + \frac{K_i^{\mathrm{v}}}{s}, \tag{3}$$

$$H_{\mathrm{LPF}} = \frac{\omega^2_{\mathrm{LPF}}}{s^2 + 2\varsigma\omega_{\mathrm{LPF}}s + 1}. \tag{4}$$

The virtual impedance can be considered as an emulation of the impedance of a traditional SM. The current reference can be calculated by:

$$\begin{bmatrix} i_d^* \\ i_q^* \end{bmatrix} = \frac{1}{r^2_{\mathrm{VSM}} + \omega^2_{\mathrm{VSM}}l^2_{\mathrm{VSM}}}\begin{bmatrix} r_{\mathrm{VSM}} & \omega_{\mathrm{VSM}}l_{\mathrm{VSM}} \\ -\omega_{\mathrm{VSM}}l_{\mathrm{VSM}} & r_{\mathrm{VSM}} \end{bmatrix} e^{dq}(s) \tag{5}$$

The control structure of the voltage control and virtual impedance is shown in Fig. 3. The tuning of r_{VSM} and l_{VSM} is explained in [18].

C. Direct Current Limitation

Direct current limitation is commonly applied in cascaded voltage and current vector controllers. Since the maximum current capacity is limited, the available current should be shared among active and reactive power. Besides, recent grid code updates for grid-forming converters further emphasise that, in voltage-source mode, current prioritisation should be guided by voltage support objectives rather than by current injection. In this context, two practical strategies have emerged: voltage symmetry priority (VSP), which favours restoring phase balance by prioritising negative-sequence reactive current, and voltage magnitude priority (VMP), which focuses on recovering positive-sequence voltage magnitude before addressing unbalance [19].

Assuming the unconstrained positive- and negative-sequence current references are $\mathbf{i}_1 = \begin{bmatrix} i_{1d} & i_{1q} \end{bmatrix}^T$ and $\mathbf{i}_2 = \begin{bmatrix} i_{2d} & i_{2q} \end{bmatrix}^T$, the sequence magnitudes are written as:

$$I_1 = \sqrt{i_{1d}^2 + i_{1q}^2}, \quad I_2 = \sqrt{i_{2d}^2 + i_{2q}^2}. \tag{6}$$

The limited references (i_{1d}^*, i_{1q}^*, i_{2d}^*, i_{2q}^*) are calculated so that $I_1^* + I_2^* \leq I_{\max}$. As a result, the direct current limiter can be classified as follows [19], [20].

1) **RP** - Reactive priority: the converter capacity is allocated first to the reactive power and proportionally between positive- and negative-sequences.

$$\begin{cases} \beta & = \min\left(1, \frac{I_{\max}}{I_1+I_2}\right) \\ i_{1q}^* & = \beta\, i_{1q}^{\mathrm{ref}}, \quad i_{2q}^* = \beta\, i_{2q}^{\mathrm{ref}} \\ i_{1d}^* & = \max\left(0, \sqrt{(\beta I_1)^2 - i_{1q}^{*2}}\right) \\ i_{2d}^* & = \max\left(0, \sqrt{(\beta I_2)^2 - i_{2q}^{*2}}\right) \end{cases} \tag{7}$$

2) **AP** - Active priority: the converter capacity is allocated first to the active power and proportionally between positive- and negative-sequences.

$$\begin{cases} i_{1d}^* & = \beta\, i_{1d}^{\mathrm{ref}}, \quad i_{2d}^* = \beta\, i_{2d}^{\mathrm{ref}} \\ i_{1q}^* & = \max\left(0, \sqrt{(\beta I_1)^2 - i_{1d}^{*2}}\right) \\ i_{2d}^* & = \max\left(0, \sqrt{(\beta I_2)^2 - i_{2q}^{*2}}\right) \end{cases} \tag{8}$$

3) **NP** - Non-priority: the current is limited with the same scales among dq components and sequences.

$$\mathbf{i}_1^* = \beta\, \mathbf{i}_1^{\mathrm{ref}}, \quad \mathbf{i}_2^* = \beta\, \mathbf{i}_2^{\mathrm{ref}}. \tag{9}$$

4) **VSP** - Voltage symmetry priority: the converter capacity is allocated first to the active power in the negative-sequence to suppress negative-sequence voltage [19].

$$\begin{cases} I_2^* = \min\left(I_2, I_{\max}\right), \quad I_1^* = \sqrt{(I_{\max}^2) - I_2^{*2}} \\ i_{2q}^* = \min\left(i_{2q}, I_2^*\right), \quad i_{1q}^* = \min\left(i_{1q}, I_1^*\right) \\ i_{2d}^* = \max\left(0, \sqrt{I_2^{*2} - i_{2q}^{*2}}\right) \\ i_{1d}^* = \max\left(0, \sqrt{I_1^{*2} - i_{1q}^{*2}}\right) \end{cases} \tag{10}$$

5) **VMP** - Voltage magnitude priority: the converter capacity is allocated first to the active power in the positive-sequence to improve positive-sequence voltage [19].

$$\begin{cases} I_1^* = \min\left(I_1, I_{\max}\right), \quad I_2^* = \sqrt{(I_{\max}^2) - I_1^{*2}} \\ i_{1q}^* = \min\left(i_{1q}, I_1^*\right), \quad i_{2q}^* = \min\left(i_{2q}, I_2^*\right) \\ i_{1d}^* = \max\left(0, \sqrt{I_1^{*2} - i_{1q}^{*2}}\right) \\ i_{2d}^* = \max\left(0, \sqrt{I_2^{*2} - i_{2q}^{*2}}\right) \end{cases} \tag{11}$$

III. Grid Code Specifications for Grid Forming

Recent grid codes and technical specifications increasingly define explicit behaviour for grid-forming (GFM) converters under faults, extending beyond the grid-following focus on simple reactive current support:

1) **Voltage support as a primary objective:** GFMs must maintain an internal voltage reference and support the positive-sequence grid voltage during and after faults, behaving as a voltage source behind an impedance (e.g., NGESO GC0137, NERC, VDE FNN) [7], [11]–[13].
2) **Fast fault-current injection (FFCI):** Current response is required within a few milliseconds after a voltage depression (e.g., GC0137 $\sim$5 ms initiation, NERC $\sim$30 ms full response) to sustain bus voltage and provide clear fault signals [7].
3) **Negative-sequence reactive current:** GFMs should supply negative-sequence reactive current during unbalanced faults when capacity allows to reduce voltage asymmetry.
4) **Voltage-based current prioritisation:** When current limiting occurs, priority should be given to supporting voltage magnitude or symmetry [9].

While these requirements define the desired external behaviour, their fulfilment depends strongly on the internal control design of the converter. In the following case study, the voltage support effects under different current limitation strategies, RP, AP, NP, VMP, and VSP, are compared to provide practical guidance for designing current limiters and virtual impedance so as to improve both voltage magnitude and symmetry during AC faults. Key control parameters influencing the rise time of fault current injection are examined to assess the feasibility of the fast response targets specified in recent grid-forming grid codes.

IV. Case Study

A. System Under Study

The system under study (Fig. 4) is an MMC with an AC line connected to a grid, which is representative of the interface of an HVDC line with an AC grid. The overall control system of MMC is detailed in Fig. 4, including an outer control loop for grid-forming functionalities, internal energy control, a state-space-based current controller, and modulation. The parameters of the system are shown in Table I. In order to evaluate the performance oft he converter during faults, time-domain simulations are performed. In the presented cases, a phase-A-to-B-ground (ABG) fault is evaluated on the transmission line at 1.5 s at 90% of the line away from the MMC.

979-8-3315-8138-1

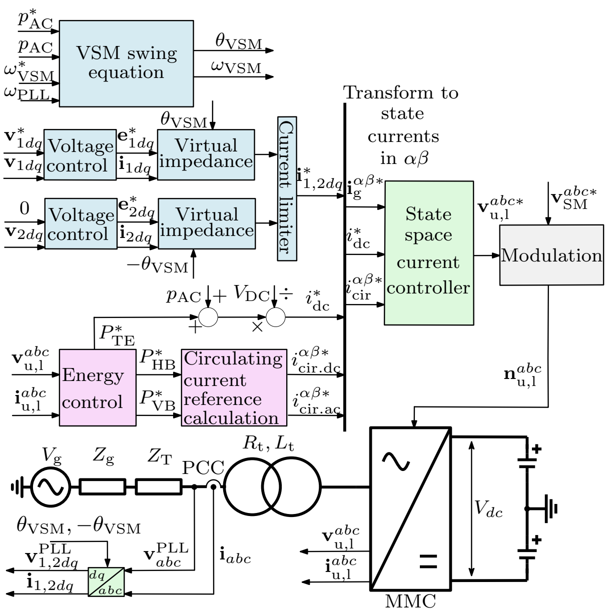

Fig. 4. System under study and overall control

TABLE I
PARAMETERS OF THE SIMULATION MODEL

Parameter name	Parameter value
Rated power	2000 MW
AC-side voltage of G2	380 kV
DC-side voltage	± 525 kV
Transformer impedance	0.002+j0.08 pu
SCR of AC grid	3
Transmission line length	50 km
Transmission line parameters	0.0126+j0.254 Ω/km
Arm reactor impedance	0.005+j0.1 pu
Phase reactor impedance	j0.05 pu
Number of arm SMs	400
SM capacitance	10 mF

B. Voltage Support Effect Under AC Faults

To quantify voltage imbalance, the ratio of the negative- to positive-sequence voltage components is used:

$$\mathrm{VUF} = \frac{V_2}{V_1} \times 100\%, \tag{12}$$

where

$$V_1 = \sqrt{v_{1d}^2 + v_{1q}^2}, \qquad V_2 = \sqrt{v_{2d}^2 + v_{2q}^2} \tag{13}$$

are the RMS magnitudes of the positive and negative sequence voltages at the PCC. The *voltage unbalance factor (VUF)* directly reflects how effectively the converter reduces negative-sequence content and restores phase symmetry during and after a fault. For *voltage magnitude support*, the positive-sequence magnitude V_1 is monitored. These metrics (VUF and normalized V_1) allow direct assessment of whether a given current limitation and virtual impedance design achieves the required *voltage symmetry* and *voltage magnitude support* specified for grid-forming converters under AC fault conditions.

The voltage performance during the fault obtained with different current limitation strategies and virtual impedance ratios (the ratio between X and R) is compared in Fig. 5–Fig. 6. The impact of different current limitations is more significant than the ratio of virtual impedance. The maximum voltage imbalance during the time window 1.50–1.70 s (Fig. 5) shows that the AP strategy leads to higher imbalance (higher than 125%) due to no reactive current injection. Among all other current limiters which injects reactive current, VSP clearly reduces the most voltage imbalance level to 80% - 100%, while the effect of RP, NP, and VMP on voltage balance prioritisation shows similar level. Decreasing the virtual impedance ratio further suppresses imbalance for VSP but has limited benefit when using RP, AP, or NP.

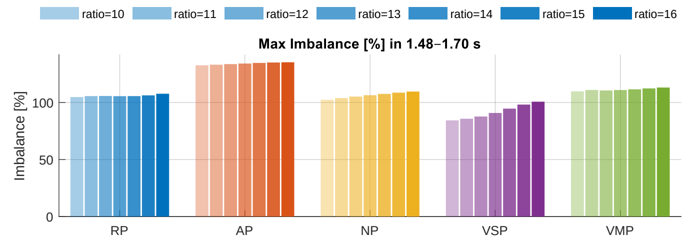

Fig. 5. Maximum voltage imbalance with different current limiters and virtual impedance ratios

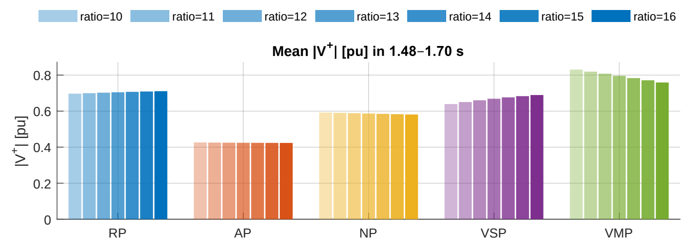

Fig. 6. Magnitude of positive-sequence voltage with different current limiters and virtual impedance ratios

The mean positive-sequence voltage magnitude $|V_1|$ over the same time interval (Fig. 6) shows that the VMP consistently yields the highest V_1 support, while RP and VSP provide only partial support. NP performs moderately but remains inferior to RP and VSP as it still remains partially active current. These results highlight that prioritising current based on voltage characteristics (VSP or VMP) provides a clear advantage over conventional RP, AP, or NP strategies in meeting voltage support requirements under AC faults.

C. Rise Time of Current Injection

The transient response of the negative-sequence reactive current components i_{1q} (solid line) and i_{2q} (dashed line) during an ABG fault for different low-pass filter bandwidth ω_{LPF} and proportional gains K_p^{v} of the voltage controller are shown in Fig. 7. The effect of varying ω_{LPF} for fixed K_p^{v} values are shown in Fig. 7 (a) and (b). A higher ω_{LPF} (faster voltage feedback) leads to a steeper initial current rise but also produces larger oscillations and overshoot, indicating a possible instability issue during fault recovery as illustrated by the yellow dashed line in Fig. 7 (b). Conversely, a lower ω_{LPF} results in a slower but more damped current injection. The impact of increasing K_p^{v} for fixed ω_{LPF} is shown in Fig. 7(c) and (d). Larger K_p^{v} strengthens the voltage regulation loop, improving the initial current injection capability but

979-8-3315-8138-1

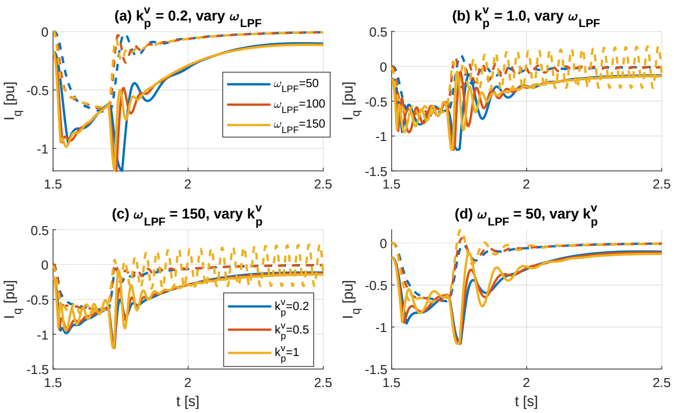

Fig. 7. $i_{1,2q}$ under ABG fault with different ω_{LPF} and K_p^{v}.

also amplifying transient oscillations if not adequately filtered. These results highlight that the rise time and damping of fault current injection are highly sensitive to the combined tuning of ω_{LPF} and K_p^{v}. Therefore, a balanced choice is required to achieve a fast response while avoiding control instability.

The rise time of the reactive current ranges from 27.95 ms (yellow solid line in Fig. 7 (a)) to 69.35 ms (blue dashed line in Fig. 7 (a)), which is far from the expectations of the present grid code (5 to 10 ms). Therefore, an injection rise time of 5 ms might be unrealistic because lower ω_{LPF} and faster voltage control (larger K_p^{v}) might cause instability as shown in Fig. 7 (b) and Fig. 7 (c). Consequently, compliance targets should be framed as an admissible range (with explicit stability margins) and verified through a co-design of ω_{LPF}, K_p^{v}, virtual-impedance parameters, and current-limiting logic.

V. Conclusion

This paper has investigated the fault response of grid-forming converters with a focus on current limitation and voltage support. The results show that defining current allocation by *positive* and *negative* sequence components is more effective than traditional active/reactive partitioning. To enhance *voltage symmetry*, negative-sequence reactive current should be prioritised, while positive-sequence support is preferable for restoring *voltage magnitude*. Allocating current to active power is counterproductive under fault conditions. Moreover, very fast fault current injection targets (e.g., 5–10 ms) are often impractical and risk instability unless the virtual impedance, low-pass filtering, and voltage control bandwidth are co-designed. These insights provide practical guidance for designing current limiters and tuning voltage control to ensure stable and grid-code-compliant performance.

References

[1] M. Bahrman, B. Johnson, "The ABCs of HVDC transmission technologies," *IEEE Power Energy Mag.*, vol. 5, no. 2, pp. 32–44, March 2007.

[2] Y. Li, Y. Gu and T. C. Green, "Revisiting Grid-Forming and Grid-Following Inverters: A Duality Theory," *IEEE Trans. on Power Syst.*, vol. 37, no. 6, pp. 4541-4554, Nov. 2022.

[3] R. Rosso, X. Wang, M. Liserre, X. Lu and S. Engelken, "Grid-Forming Converters: Control Approaches, Grid-Synchronization, and Future Trends—A Review," *IEEE Open J. Ind. Appl.*, vol. 2, pp. 93-109, 2021.

[4] ENTSO-E, "The Network Code on High Voltage Direct Current Connections (HVDC)", Brussels, 2016. [online]. Available: https://www.entsoe.eu/network_codes/hvdc/

[5] Rüberg S, Sewdien V, Rueda Torres JL, Rakhshani E, Wang D, Tuinema B, et. al, "Deliverable D1.6 Demonstration of Mitigation Measures and Clarification of Unclear Grid Code Requirements", 2019. 172 S. [online]. Available: https://www.fis.uni-hannover.de/portal/de/publications/deliverable-d16-demonstration-of-mitigation-measures-and-clarification-of-unclear-grid-code-requirements(2802129c-369b-4fd8-a0d8-5773807a7a57).html

[6] UNIFI Consortium, "Grid-forming Inverter Technology Specifications: A Review of Research Reports and Roadmaps," UNIFI, 2022. [Online]. Available: https://www.researchgate.net/publication/365687427_Grid-forming_Inverter_Technology_Specifications_Grid-forming_Inverter_Technology_Specifications_A_Review_of_Research_Reports_Roadmaps.

[7] National Grid Electricity System Operator (NGESO), "Grid Code Modification GC0137: Minimum Specification Required for Provision of GB Grid Forming Capability," 2021. [Online]. Available: https://www.neso.energy/document/189381/download

[8] Australian Energy Market Operator (AEMO), "Voluntary Specification for Grid-Forming Inverters: Core Requirements and Test Framework," 2023. [Online]. Available: https://aemo.com.au/initiatives/trials/grid-forming-inverters

[9] European Network of Transmission System Operators for Electricity (ENTSO-E), "Grid Forming Capability of Power Park Modules: First Interim Report on Technical Requirements," 2024. [Online]. Available: https://www.entsoe.eu/Documents/Publications/SOC/20240503_First_interim_report_in_technical_requirements.pdf

[10] Agency for the Cooperation of Energy Regulators (ACER), "Recommendation No 03/2023 on the Grid-Forming Capability of Inverter-Based Resources," 2023. [Online]. Available: https://acer.europa.eu/Official_documents/Acts_of_the_Agency/Recommendations/ACER%20Recommendation%2003-2023.pdf

[11] Verband der Elektrotechnik Elektronik Informationstechnik e.V. (VDE FNN), "Technische Anforderungen an netzbildende Eigenschaften inklusive der Bereitstellung von Momentanreserve," 2024. [Online]. Available: https://www.vde.com/de/fnn

[12] North American Electric Reliability Corporation (NERC), "Grid Forming Functional Specifications for Bulk Power System-Connected Battery Energy Storage Systems," 2023. [Online]. Available: https://www.nerc.com/comm/RSTC_Reliability_Guidelines/White_Paper_GFM_Functional_Specification.pdf

[13] U.S. Department of Energy (DOE), "Specifications for Grid-Forming Inverter-Based Resources," 2023. [Online]. Available: https://www.energy.gov/sites/default/files/2023-09/Specs%20for%20GFM%20IBRs%20Version%201.pdf

[14] N. Mohammed, H. Udawatte, W. Zhou, D. J. Hill and B. Bahrani, "Grid-Forming Inverters: A Comparative Study of Different Control Strategies in Frequency and Time Domains," *IEEE Open J. Ind. Electron. Soc.*, vol. 5, pp. 185-214, 2024,

[15] N. Baeckeland, D. Chatterjee, M. Lu, B. Johnson and G. -S. Seo, "Overcurrent Limiting in Grid-Forming Inverters: A Comprehensive Review and Discussion," *IEEE Trans. on Power Electron.*, vol. 39, no. 11, pp. 14493-14517, Nov. 2024.

[16] S. Ramachandra, K. Dey, A. M. Kulkarni, and A. M. Gole, "Angular stability of grid forming converters subjected to large disturbances," in *Proc. 16th Int. Conf. on Power Systems Transients (IPST)*, Mexico City, Mexico, 2025.

[17] Y. Khayat, P. Chen, M. Bongiorno, B. Johansson and R. Majumder, "FRT Capability of Grid-Forming Power Converters: An Antiwindup Scheme," *IEEE Trans. on Power Electron.*, vol. 39, no. 10, pp. 12842-12855, Oct. 2024

[18] H. Wu and X. Wang, "Control of Grid-Forming VSCs: A Perspective of Adaptive Fast/Slow Internal Voltage Source," *IEEE Trans. on Power Electron.*, vol. 38, no. 8, pp. 10151-10169, Aug. 2023.

[19] Tavakoli, S.D., Prieto-Araujo, E., Gomis-Bellmunt, O., Galceran-Arellano, S., "Fault ride-through control based on voltage prioritization for grid-forming converters," *IET Renew. Power Gener.*, vol. 17, pp. 1370-1384, 2023.

[20] X. Liu, P. Judge, G. Chaffey, W. Leterme and D. Van Hertem, "Impact of Current Limiter Implementation in MMC Control on AC Fault-Ride-Through and System Distance Protection," *2024 Energy Conversion Congress & Expo Europe (ECCE Europe)*, Darmstadt, Germany, 2024.

979-8-3315-8138-1